pH of Aerosols in a Polluted Atmosphere: Source Contributions to Highly Acidic Aerosol

Guoliang Shi [†,§*], Jiao Xu [†], Xing Peng [†], Zhimei Xiao [‡], Kui Chen [‡],

Yingze Tian [†], Xinbei Guan [§], Yinchang Feng [†], Haofei Yu [§], Athanasios Nenes [‖],

Armistead G. Russell [§*]

[†] State Environmental Protection Key Laboratory of Urban Ambient Air Particulate Matter Pollution Prevention and Control, College of Environmental Science and Engineering, Nankai University, Tianjin, 300071, China

[‡] Environmental Monitoring Center of Tianjin

[§] School of Civil and Environmental Engineering, Georgia Institute of Technology, Atlanta, Georgia 30332-0512

[‖] Earth and Atmospheric Sciences, Georgia Institute of Technology, Atlanta, GA 30332

∗Corresponding Author: Phone: +86 22 23507962. Fax: +86 2223503397. E-mail: nksgl@nankai.edu.cn, ted.russell@gatech.edu

Summary

26 Pages, 11 Figures and 4 Tables

Table S1. Concentrations of WS-ions during the sampling period (μg m^{-3})
Table S2. Regression information for AE and CE against source contributions (μg m^{-3})
Table S3. Regression information for Neutralization ratio $R_{neutral}$ against source contributions (μg m^{-3})
Table S4. Regression information for ΔpH, pH and 10^{pH} against source contribution (μg m^{-3})

Concentrations and Existing Forms of WS-ions. In this study, the hourly concentrations of total WS-ions species in the collected $PM_{2.5}$ samples ranged from 2.8 μg m^{-3} to 401.9 μg m^{-3} with an average level of 37.01 μg m^{-3}. As shown in Table S1, ions with the highest average concentrations are ranked as: NO_3^- (10.7 μg m^{-3}), SO_4^{2-} (8.9 μg m^{-3}), NH_4^+ (6.9μg m^{-3}), Cl^- (3.5μg m^{-3}), K^+ (1.3μg m^{-3}), F^- (0.9 μg m^{-3}), Na^+ (0.9 μg m^{-3}), Ca^{2+} (0.5 μg m^{-3}) and Mg^{2+} (0.1 μg m^{-3}). Among them SO_4^{2-}, NO_3^- and NH_4^+ are the three dominant species, accounting for approximately 78% of total $PM_{2.5}$ mass, a similar percentage also found in other studies[1]. The average concentrations of Cl^-, F^-, NO_2^-, Mg^{2+}, K^+, Na^+ and Ca^{2+} together account for 22% of the measured WS-ions concentrations.

Concentration variations (μg m^{-3}) of the three dominant components (NH_4^+, SO_4^{2-} and NO_3^-) are shown in Figure. 1. NH_4^+ is the dominant cation component, with an average concentration value of 6.9 μg m^{-3}. During the sampling period, average NH_4^+ concentrations are higher in heating period (8.7 μg m^{-3}) than non-heating period (4.8 μg m^{-3}). The seasonal trends of the other two major ions, $NO_3^-$and SO_4^{2-}, are similar with NH_4^+, with average concentration levels higher in heating period (13.5 μg m^{-3} and 10.2 μg m^{-3}, respectively), and lower in summer time (non-heating period, 7.6 μg m^{-3} and 7.4 μg m^{-3}, respectively). Temporal concentration variations of dominant WS-ions in this study are consistent with results from other studies. For example, Zhang et al. (2011) found that the above mentioned three major species accounted for 82% of total WS-ions concentrations, and NO_3^- and NH_4^+

concentrations peak in winter and are lower in spring[1].

Nitrate and sulfate are the two major anion components in Tianjin during the sampling period. Studies have shown that particulate nitrate is formed through the photo-oxidation of NO_2 emitted from fossil fuels combustion[1, 2, 3], and sulfate can be formed by the oxidization of SO_2 through heterogeneous or homogeneous reactions[4, 5]. Ammonium is the dominant cation in the collected particulate matter. The most possible solute species in this study include ammonium chloride (NH_4Cl), ammonium nitrate (NH_4NO_3) and ammonium sulfate ($(NH_4)_2SO_4$). Studies showed that ammonium chloride is the most volatile among the three; ammonium nitrate is thermally instable; and ammonium sulfate is the most stable. Thus, ammonium preferably bind with sulfate first, then nitrate, followed by other anions such as nitrite or chloride[6, 7, 8, 9].

The formation of $(NH_4)_2SO_4$ and NH_4NO_3 are influenced by concentrations of participating species as well as atmospheric conditions such as temperature and relative humidity. Plots of ammonium and sulfate & nitrate (in equivalent unit) are provided in Figure. S1. A close to 1 ratio of ammonium equivalents to nitrate and sulfate equivalents ($E_{ammonium}/E_{nitrate+sulfate}$) suggests that all of the ammonium ions might be neutralized by sulfate and nitrate ions, indicating the predominance of ammonium sulfate ($(NH_4)_2SO_4$) and ammonium nitrate (NH_4NO_3) as ammonium salt in particulate matter[10, 11]. A larger than 1 ratio indicating the existence of other

ammonium salts in addition to ammonium sulfate and ammonium nitrate; and a lower than 1 ratio may be due to that all of the ammonium were neutralized by sulfate and nitrate, and other sulfate salt or nitrate salt may also exist. Figure. S1 also illuminates correlation plots of $E_{ammonium}$ against $E_{nitrate+sulfate}$ for different seasons (heating and non-heating season). The plots were separated into two groups manually, one is the ratios higher than 1, the other group is the ratios lower than 1 (Figure. S1). Overall, ammonium fractions are higher in heating than non-heating period. Although, in a small number of days in the heating period, ammonium concentrations are not as high, which may be due to special source contributions and/or meteorological conditions.

Source Analysis for WS-ions. As shown in Figure. S2, the AE-CE plots for two periods show different patterns, suggest different emission source contributions of WS-ions in the two periods. To further investigate this issue, the hourly online measurement dataset (2971×12: 2971 samples and 12 species) were analyzed by ME2 to identify potential sources. The dataset contains mass concentrations of all particulate ion components (NH_4^+, Na^+, K^+, Ca^{2+}, Mg^{2+}, SO_4^{2-}, NO_3^-, Cl^-) as well as gaseous pollutants (SO_2, NO_2, CO). Concentrations of SO_2 and NO_2 were down weighted (by a factor of 100) to reduce their impacts on factor profiles. Five factors were extracted from the ME2 modeling, with a Q value of 22515 (Q_{main}= 21208, Q_{aux}= 1307, Q_{aux}/Q_{main}=6%), which is close to the theoretical Q value (20737: $2971\times12-5\times(2971+12)$), indicated satisfactory model performance. Generally,

Q_{aux} indicates the residual error which caused by factor pulling, the ratio of Q_{aux}/ Q_{main} can indicate the uncertainties involved in factor pulling. A ratio less than 15% is desirable.

The extracted source profiles are shown in Figure. S3. Factor 1 showed high loadings for Cl^-, NH_4^+, and SO_2. According to previous studies, Cl^- was an important marker of coal combustion[9, 12, 13]. In the study region, coal combustions are also accompanied by emissions of SO_2. Therefore, this factor was identified as coal combustion source.

Factor 2 was weighted by Ca^{2+}, Mg^{2+}, which were considered as markers of mineral dust, hence this factor was identified as mineral dust source[14]. It is known that mineral dusts may come from both natural origin (natural soil dust) and human activities (e.g. road dust and construction dust). It should be noted that, during the study period, the city of Tianjin has an overall construction area of 215.2 million m^2, concentrated in urbanized regions. Similar results can also be found in other studies such as Song et al. (2006)[15], who found that mineral dust source contribute significantly to ambient $PM_{2.5}$ in northern China.

Factor 3 show high loadings of NO_2 and CO, which are likely to be emitted by vehicles. Therefore, this factor was identified as vehicle exhaust source[14, 16, 17]. As of 2014, the total vehicle population in Tianjin has reached 2.88 million, which ranked

89 seventh place in China according to Tianjin Statistical Yearbook (2015)[18]. This
90 enormous vehicle fleet emitted large amount of secondary PM precursors such as
91 SO_2 and NO_x, which triggers significant regulatory concerns.
92
93 Factor 4 shows high loadings for NO_3^- and NH_4^+, which can be identified as
94 secondary nitrate source. Factor 5 is weighted by SO_4^{2-} and NH_4^+, and was treated as
95 secondary sulfate source. It is well acknowledged the formations of secondary nitrate
96 and sulfate sources are contributed by their gaseous precursors species such as NO_x
97 and SO_2[19, 20], which are emitted from vehicles, fossil fuel, coal combustion and
98 industry process[21]. As one of the largest cities in China, Tianjin has great numbers of
99 gaseous precursor sources, including heavy traffic emissions, large amount of coal
100 combustion activities as well as many industrial factories. According to Tianjin
101 Statistical Yearbook (2015)[18], annual emissions of SO_2 and NO_x in Tianjin are close
102 to half million tons in 2014. These large amount of emissions of precursors are likely
103 to contribute to the formation of secondary sulfate and nitrate sources.
104
105 To assess the performance of the ME2 model, the model estimated $PM_{2.5}$
106 concentrations were compared with measured $PM_{2.5}$ mass concentrations. The
107 estimated mass concentrations of $PM_{2.5}$ were calculated according to Eq (S1):

108 $$Mass_i = \sum_{p=1}^{P} Con_{pi} \quad \text{(S1)}$$

109 where, $Mass_i$ is the estimated $PM_{2.5}$ concentration of the *i*th sample; Con_{pi} is the

estimated contribution (by ME2) of the *p*th sources to receptor in the *i*th sample; and *P* is the total number of extracted source categories.

The fitting plot between measured and estimated $PM_{2.5}$ concentrations is shown in Figure. S4 (three outlier point were removed). The regression intercept is 0.00 and the Pearson correlation coefficient is 0.99, indicates that the estimated $PM_{2.5}$ concentrations for most samples are close to measurement and the modeling results are satisfactory.

Impact of Sources on AE and CE. Source impact on WS-ions levels was analyzed using regression source contribution against AE (1), CE, pH, and Neutralization ratio ($R_{neutral}$) (Additional details are provided in Table S2 and S3).

AE was used as the dependent variable for regression in consideration of the linear relationship between source contributions and AE. The equation is:

$$AE = -0.036 + 0.017\ Coal + 0.010\ Dust + 0.017\ Vehicle + 0.014\ SN + 0.012\ SS \quad \text{(S2)}$$

where SN is secondary nitrate and SS is secondary sulfate. This equation has an R^2 of 0.93, indicating a linear fit. Detailed information regarding the regression are provided in Table S2. Dust has a slightly lower regression coefficient compared to other sources, which is consistent with results from other studies[22, 23].

Similarly, CE was also regressed with source contributions ($R^2 = 0.92$):

$$CE = 0.074 + 0.018\ Coal + 0.012\ Dust + 0.0044\ Vehicle + 0.0068\ SN + 0.018\ SS \quad \text{(S3)}$$

As expected, both coal and dust contribute strongly to CE, as does secondary sulfate, a finding can be explained by the association between NH_4^+ and the factor (Figure. S3).

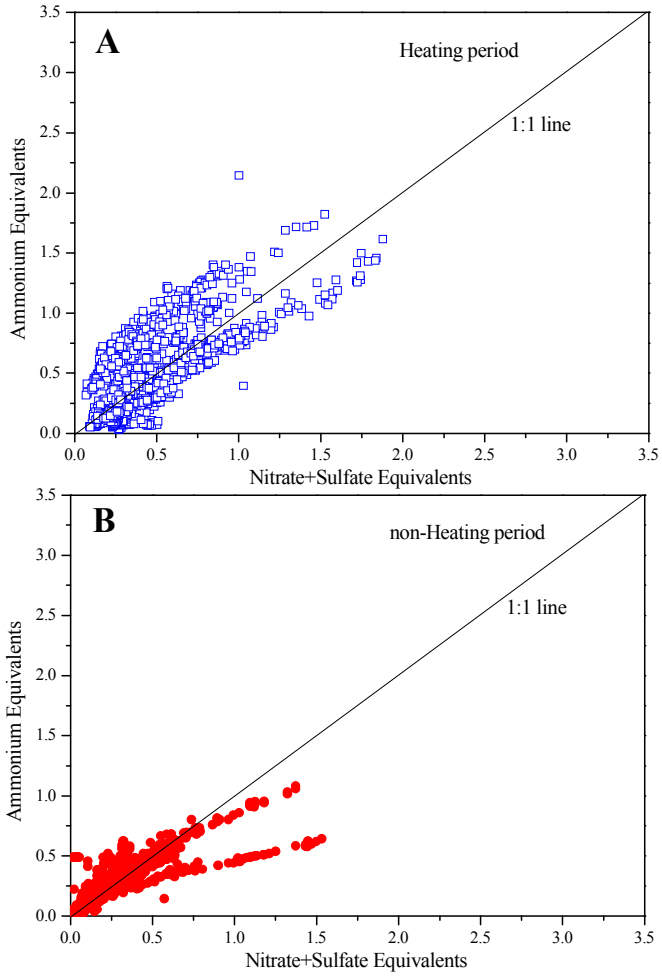

Figure S1. Relationships between ammonium vs. nitrate plus sulfate (in equivalence units) for the (a) heating and (b) non-heating periods.

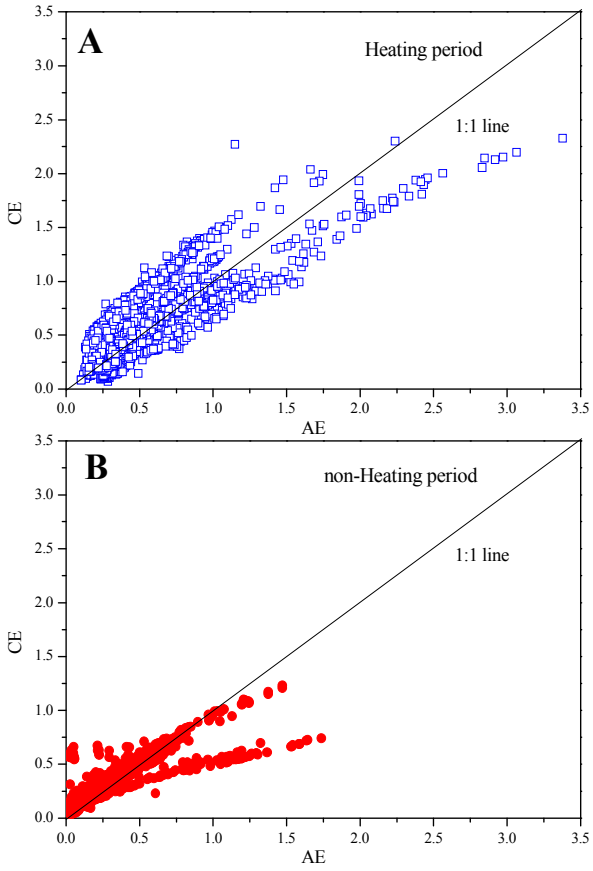

Figure S2. Relationship between AE (anion equivalent, mol m^{-3}) and CE (cation equivalent, mol m^{-3}) for (A) Heating period and (B) non-heating period. During the heating period, there are two branches: a relatively larger branch under the 1:1 line and another branch above the line; Similar pattern can also be found for the non-heating period, with one group relatively closer to the 1:1 line, and the other group above the 1:1 line. The average AE/CE ratio for all samples is 0.97.

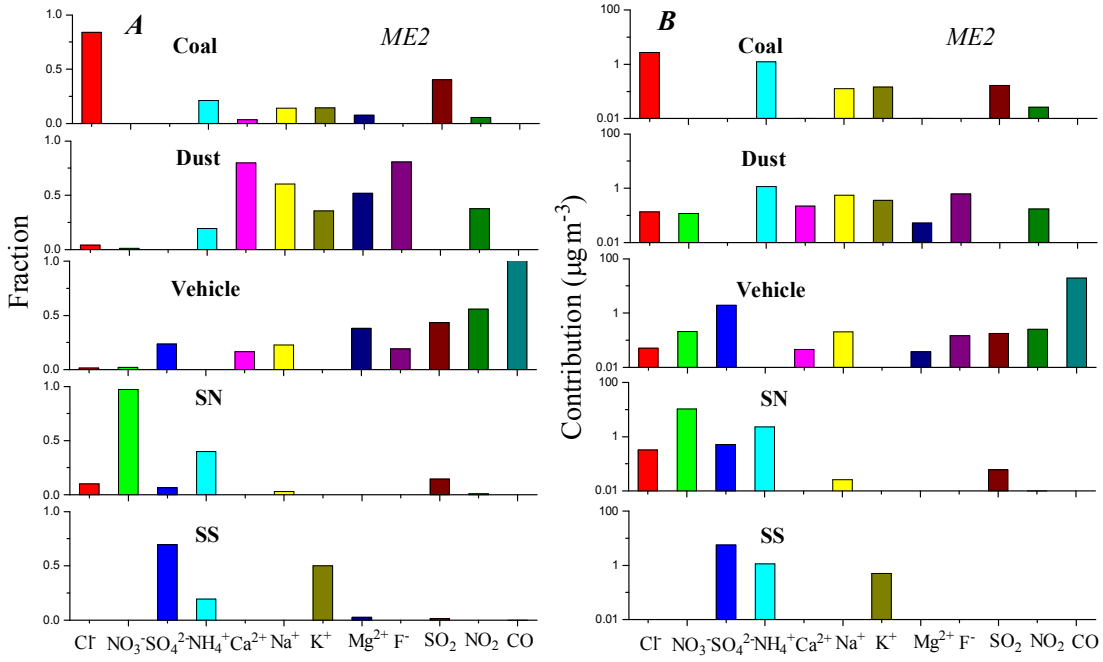

Figure S3. Profiles of five sources extracted byME2.

A: Species Fraction

The fraction is the proportion of *i*th species from one factor to the total mass of ith species in the ambient, which can be calculated as:

$$fraction_{jp} = c_{jp} / c_j^*$$

where $fraction_{jp}$ is the proportion of *j*th species from one factor to the total mass of *p*th species in the ambient; c_{jp} is the contribution (μg m^{-3}) of *j*th species from *p*th factor calculated by ME2; c_j^* is the concentration (μg m^{-3}) of *j*th species in this ambient.

B: Species Contribution

The Species Contribution is the contribution (μg m^{-3}) of individual species from each source. Note: the contributions for SO_2, NO_2 and CO were the values (bar shown in Figure S3A)×100

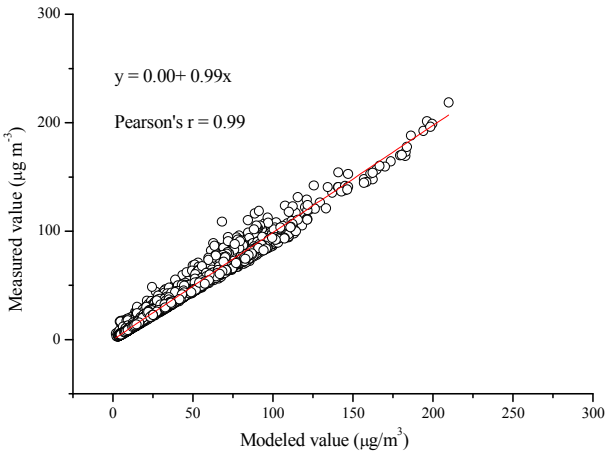

Figure S4. Fitting plot of modeled concentration and measured concentration of WS-ions. The regression intercept is 0.00 and the Pearson correlation coefficient is 0.99.

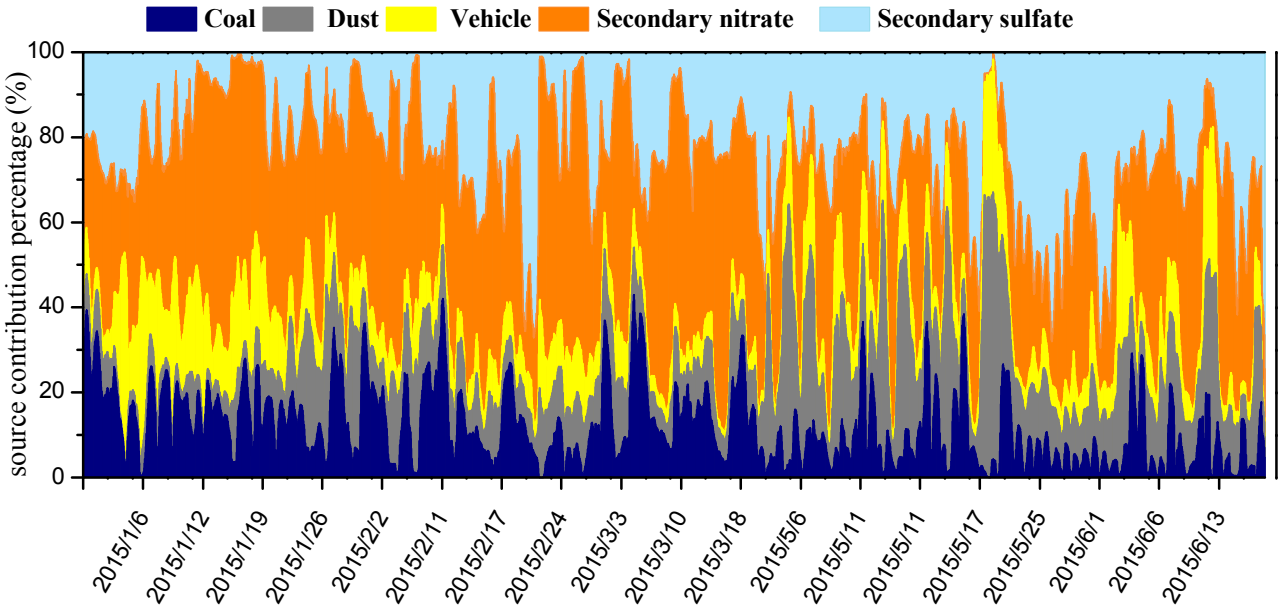

Figure S5. Time variation of five sources during the sampling period. The secondary nitrate factor represents the largest contribution, 41%, to total WS-ions; the second largest contributor is secondary sulfate (26%), followed by coal combustion (14%), mineral dust (11%) and vehicle exhaust source 9%.

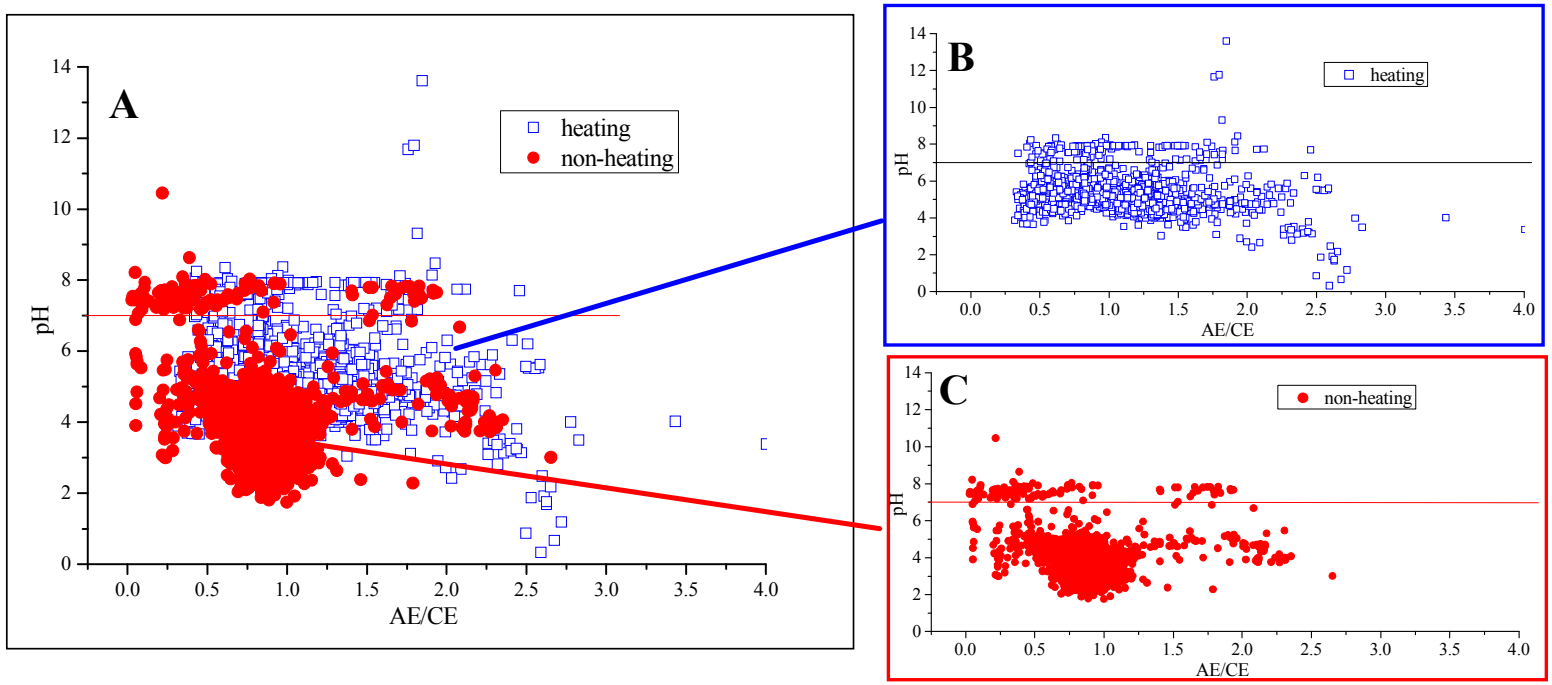

Figure S6. AE/CE-pH plots during heating and non-heating periods (A). AE/CE-pH relationships for both heating (B) and non-heating period (C) overlapped and show generally negative slopes. Such results are expected since high AE/CE ratios lead to lower pH values and low AE/CE ratios lead to higher pH values.

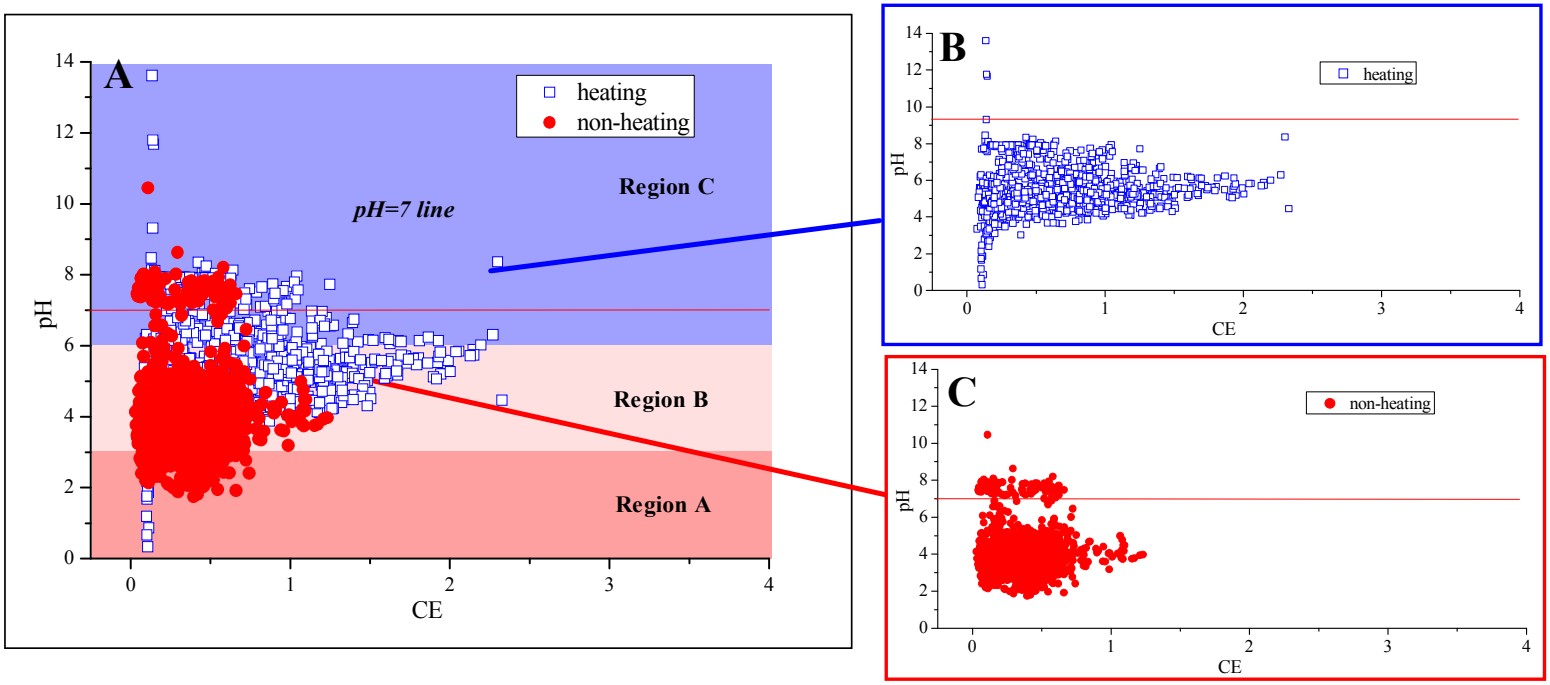

Figure S7. CE (mol m^{-3}) vs. pH levels (A), for the (B) heating and (C) non-heating periods. Region A (pH < 3, low pH region), Region B (3 < pH < 6, moderately low-pH) and Region C (pH > 6)

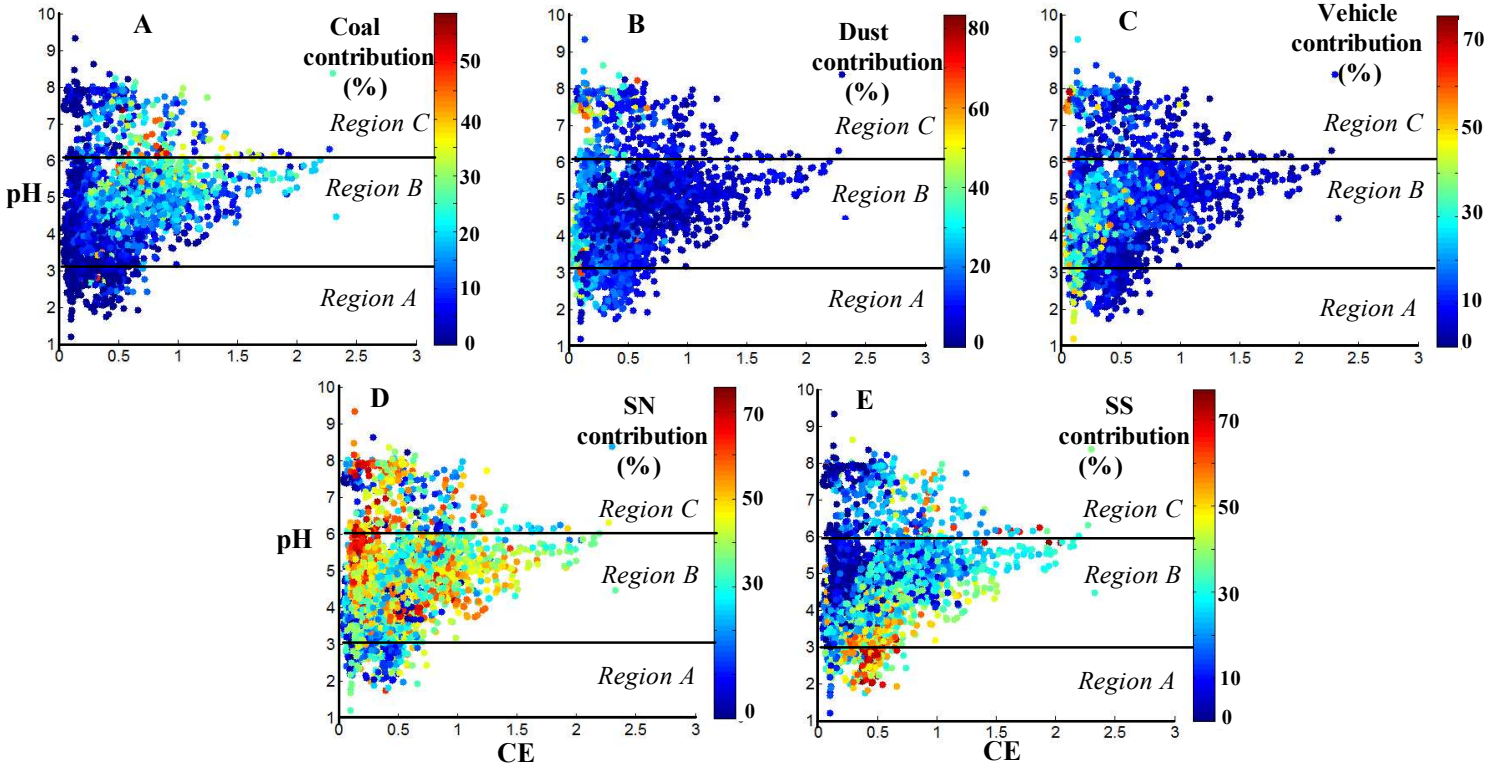

Figure S8. CE (mol m^{-3}) vs. pH, colored bar shows the percentage source contribution (%) for (A) Coal combustion, (B) Dust, (C) Vehicles, (D) Secondary nitrate (SN) and (E) Secondary sulfate (SS). For the purpose of discussion, the ranges of pHs were divided into three regions: Region A (pH < 3, low pH region), Region B (3 < pH < 6, moderately low-pH) and Region C (pH > 6 is more neutral and alkaline). The contribution (=(S_i/S_{sum} x 100%)) is the percentage contribution (%) of i'th source category to the sum of the source impacts on water soluble ions.

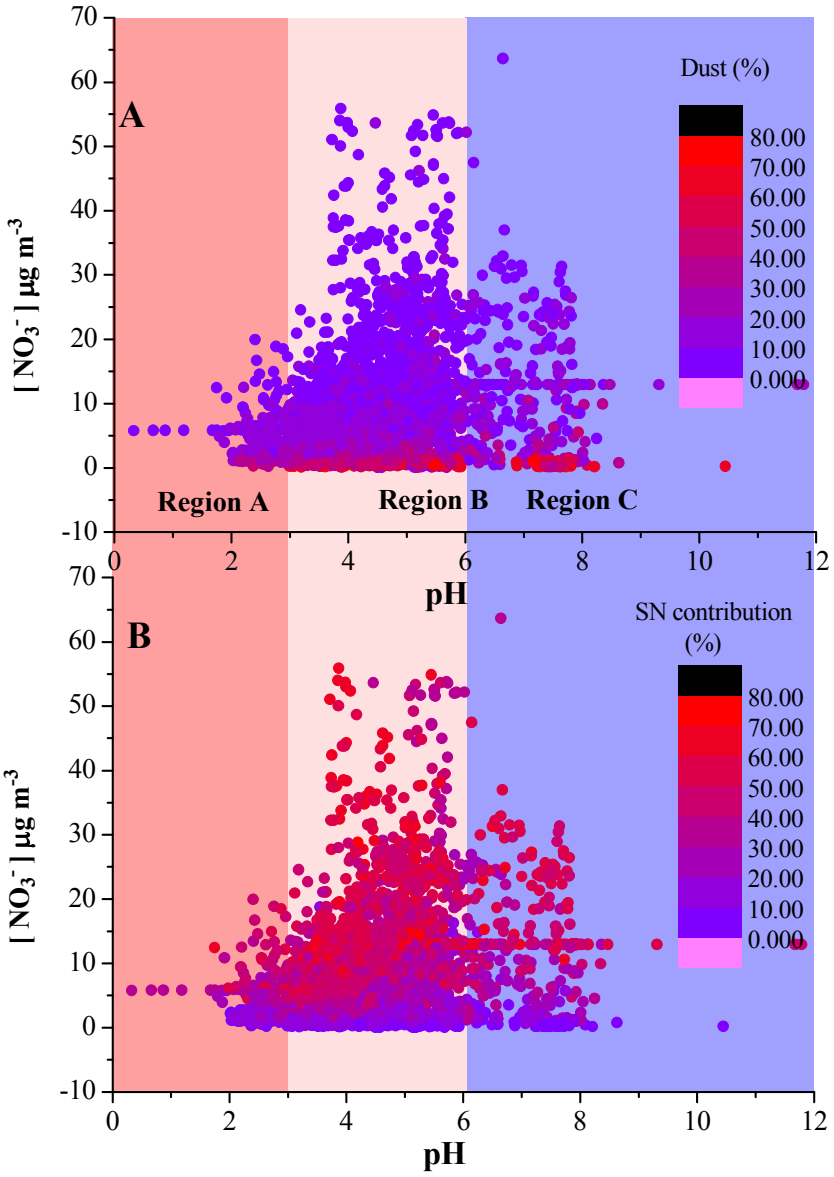

Figure S9. [NO_3^-] vs. pH. Colored bar shows the percentage source contribution (%) for (A) Dust and (B) SN (secondary nitrate). In the low-pH region, most of the NO_3^- levels are low while in Region B, NO_3^- significantly increased with pH. In the high-pH region, NO_3^- decreases while pH increases, which is linked to the samples in this region being rich in mineral dust. Region A (pH < 3, low pH region), Region B (3 < pH < 6, moderately low-pH) and Region C (pH > 6 is more neutral and alkaline). The contribution (=(S_i/S_{sum} x 100%)) is the percentage contribution (%) of i'th source category to the sum of the source impacts on water soluble ions.

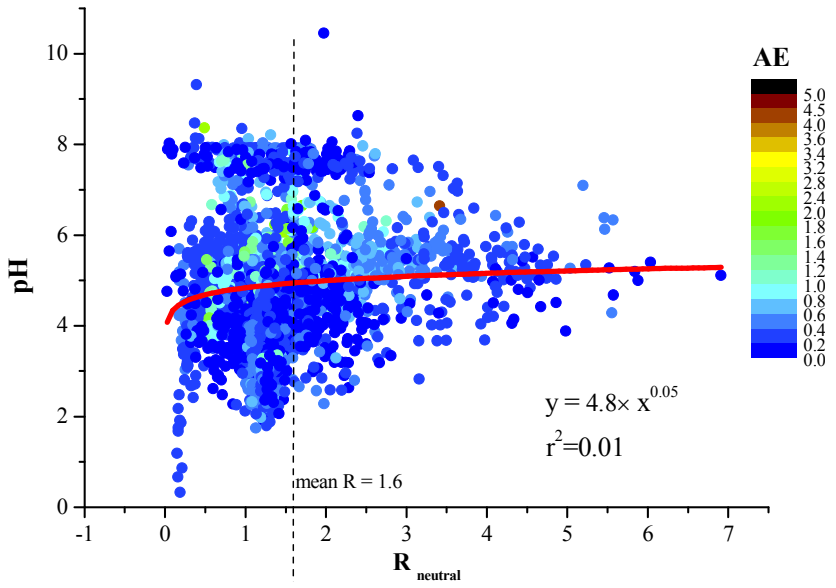

Figure S10. Neutralization ratio ($R_{neutral}$) vs. pH, colored bar shows the AE loading (anion equivalent, mol m^{-3}), $R_{neutral}$ = $[NH_4^+]$ / (2$[SO_4^{2-}]$+$[NO_3^-]$).

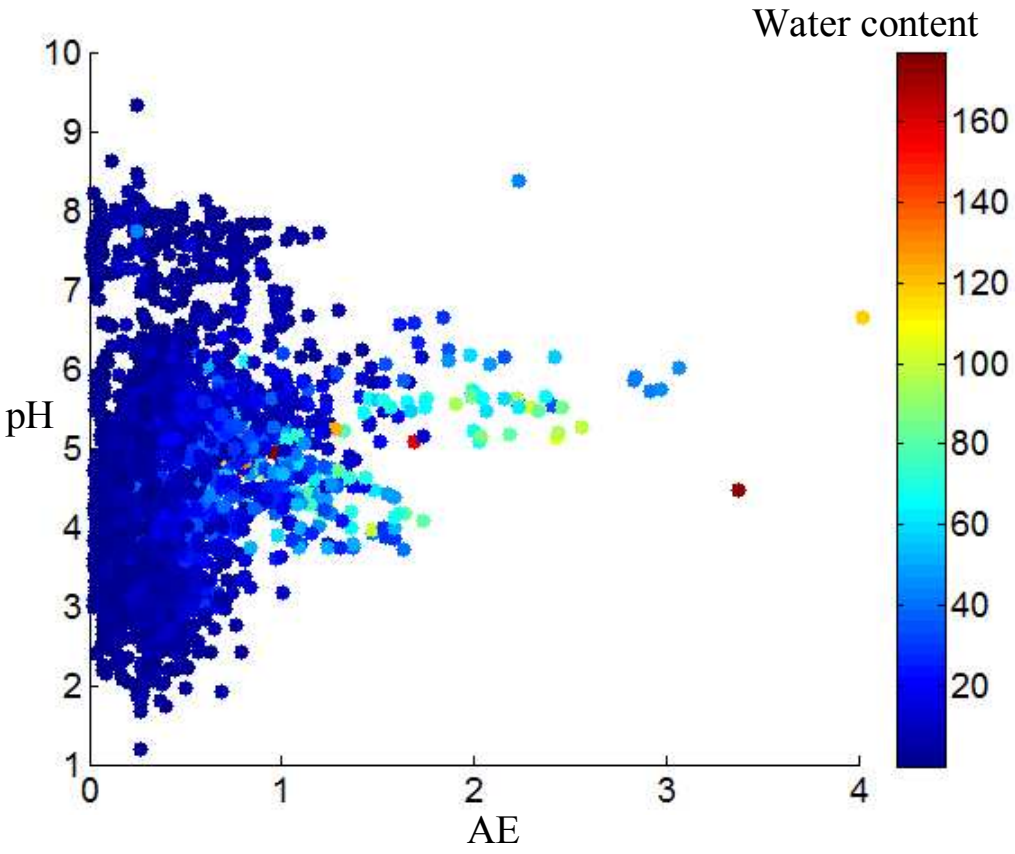

Figure S11. AE (mol m^{-3}) vs. pH, with colored bar water content (μg m^{-3}), calculated by ISORROPIA II.

Table S1. Concentrations of WS-ions during the sampling period (μg m^{-3})

Species	Whole period	Heating period	Non-heating period
NO_3^-	10.7	13.5	7.6
SO_4^{2-}	8.9	10.2	7.4
Cl^-	3.5	4.9	2.0
F^-	0.9	1.1	0.7
NH_4^+	6.9	8.7	4.8
K^+	1.3	1.6	1.0
Na^+	0.9	1.1	0.8
Ca^{2+}	0.5	0.6	0.4
Mg^{2+}	0.1	0.2	0.1

Table S2. Regression information for AE and CE against source contributions (μg m^{-3}).

	AE		CE	
	Coefficients	***Standardized Coefficients***	***Coefficients***	***Standardized Coefficients***
Constant	-0.036	0.0050	0.074	0.0080
Coal	0.017	0.00041	0.018	0.00065
Dust	0.010	0.0011	0.012	0.0017
Vehicle	0.017	0.00089	0.0044	0.0014
SN	0.014	0.00020	0.0068	0.00032
SS	0.012	0.00024	0.018	0.00038
R^2	0.93		0.80	

SN: Secondary Nitrate; SS: Secondary Sulfate.

All Coefficients are significant at the 99% confidence level.

Table S3. Regression information for Neutralization ratio $R_{neutral}$ against source contributions (μg m^{-3}).

	$R_{neutral}$	
	Coefficients	***Standardized Coefficients***
Constant	1.95	0.099
Coal	0.064	0.0081
Dust	0.051	0.021
Vehicle	-0.093	0.018
SN	-0.037	0.0039
SS	0.00047	0.0047
R^2	0.055	

SN: Secondary Nitrate;

SS: Secondary Sulfate

All Coefficients are significant at the 99% confidence level.

Table S4. Regression information for ΔpH, pH and 10^{pH} against source contribution (μg m^{-3}).

(A)	**ΔpH**	
	Coefficients	***Standardized Coefficients***
Constant	0.10	0.045
Coal	0.051	0.0037
Dust	0.095	0.0096
Vehicle	-0.070	0.0081
SN	-0.0038	0.0018
SS	-0.032	0.0022
R^2	0.16	

(B)	**pH**	
	Coefficients	***Standardized Coefficients***
Constant	4.59	0.059
Coal	0.063	0.0048
Dust	0.072	0.012
Vehicle	-0.0078	0.010
SN	0.0079	0.0023
SS	-0.043	0.0028
R^2	0.13	

(C)	**10^{pH}**	
	Coefficients	***Standardized Coefficients***
Constant	2.3×10^{10}	3.4×10^{10}
Coal	-1.2×10^{9}	2.9×10^{9}
Dust	7.5×10^{8}	7.4×10^{9}
Vehicle	1.7×10^{9}	6.2×10^{9}
SN	-2.0×10^{8}	1.4×10^{9}
SS	-8.3×10^{8}	1.7×10^{9}
R^2	0.00036	

SN: Secondary Nitrate

SS: Secondary Sulfate

All Coefficients are significant at the 99% confidence level.

References

1. Zhang, T.; Cao, J. J.; Tie, X. X.; Shen, Z. X.; Liu, S. X.; Ding, H.; Han, Y. M.; Wang, G. H.; Ho, K. F.; Qiang, J.; Li, W. T. Water-soluble ions in atmospheric aerosols measured in Xi'an, China: seasonal variations and sources. *Atmos. Res.* **2011**, *102*, 110-119.
2. Eddingsaas, N. C.; VanderVelde, D. G.; Wennberg, P. O. Kinetics and products of the acid-catalyzed ring-opening of atmospherically relevant butyl epoxy alcohols. *J. Phys. Chem. A* **114**, 8106-8113 (2010).
3. Sandford, R. C.; Exenberger, A.; Worsfold, P. J. Nitrogen cycling in natural waters using in situ, reagentless UV spectrophotometry with simultaneous determination of nitrate and nitrite. *Environ. Sci. Technol.* **2007**, *41*, 8420-8425.
4. Wang, W.; Liu, H.; Yue, X.; Li, H.; Chen, J.; Ren, L.; Tang, D.; Hatakeyama, S.; Takami, A. Study on acidity and acidic buffering capacity of particulate matter over Chinese eastern coastal areas in spring. *J. Geophys. Res.* **2006**, *111*, 4321-4344.
5. Liggio, J.; Li, S. M.; McLaren, R. Heterogeneous reactions of glyoxal on particulate matter: Identification of acetals and sulfate esters. *Environ. Sci. Technol.* **2005**, *39*, 1532-1541.
6. Tsai, J. H.; Chang, L. P.; Chiang, H. L. Airborne pollutant characteristics in an urban, industrial and agricultural complex metroplex with high emission loading and ammonia concentration. *Sci. Total Environ.* **2014**, *494-495*, 74-83.
7. Liu, S.; Hu, M.; Slanina, S.; He, L.Y.; Niu, Y. W.; Bruegemann, E.; Gnauk, Thomas.; Herrmann, Hartmut. Size distribution and source analysis of ionic compositions of aerosols in polluted periods at Xinken in Pearl River Delta (PRD) of China. *Atmos. Environ.* **2008**, *42*, 6284-6295.
8. Shi, G. L.; Liu, G. R.; Tian, Y. Z.; Zhou, X. Y.; Peng, X.; Feng, Y. C. Chemical characteristic and toxicity assessment of particle associated PAHs for the short-term anthropogenic activity event: During the Chinese New Year's Festival in 2013. *Sci. Total Environ.* **2014**, *8-14*, 482–483.
9. Hopke, P. K. Receptor Modeling in Environmental Chemistry. *John Wiley.* 1985.
10. Huang, X.; Qiu, R.; Chan, C.K.; Ravi Kant, P. Evidence of high PM2.5 strong

acidity in ammonia-rich atmosphere of Guangzhou, China: transition in pathways of ambient ammonia to form aerosol ammonium at $[NH_4^+]/[SO_4^{2-}]$= 1.5. *Atmos. Res.* **2011**, *99*, 488-495.

11. Voutsa, D.; Samara, C.; Manoli, E.; Manoli, E.; Lazarou, D.; Tzoumaka, P. Ionic composition of PM2.5 at urban sites of northern Greece: secondary inorganic aerosol formation. *Environ. Sci. Poll. Res.* **2014**, *21*, 4995-5006.
12. Gieré, R.; Smith, K.; Blackford, M. Chemical composition of fuels and emissions from a coal + tire combustion experiment in a power station. *Fuel.* **2006**, *85*, 2278-2285.
13. Nyambura, M. G.; Mugera, G. W.; Felicia, P. L.; Gathuraa, N. P. Carbonation of brine impacted fractionated coal fly ash: implications for CO_2 sequestration. *J. Environ. Manage.* **2011**, *92*, 655-664.
14. Pant, P.; Harrison, R. M. Critical review of receptor modelling for particulate matter: A case study of India. *Atmos. Environ.* **2012**, *49*, 1-12.
15. Song, Y.; Xie, S.; Zhang, Y.; Zeng, L.; Salmon, L.G.; Zheng, M. Source apportionment of PM2.5 in Beijing using principal component analysis/absolute principal component scores and UNMIX. *Sci. Total Environ.* **2006**, *372*, 278-86.
16. Li, L.; Li, M.; Huang, Z. X.; Gao, W.; Nian, H. Q.; Fu, Z.; Gao, J.; Chai, F. H.; Zhou, Z. Ambient particle characterization by single particle aerosol mass spectrometry in an urban area of Beijing. *Atmos. Environ.* **2014**, *94*, 323-331.
17. Mooibroek, D.; Schaap, M.; Weijers, E. P.; Hoogerbrugge, R. Source apportionment and spatial variability of PM2.5 using measurements at five sites in the Netherlands. *Atmos. Environ.* **2011**, *45*(25): 4180-4191.
18. Bureau, Tianjin. Tianjin Statistical Yearbook (2015).
19. Maier, M. L.; Balachandran, S.; Sarnat, S. E.; Turner, J. R.; Mulholland, J. A.; Russell, A. G. Application of an Ensemble-Trained Source Apportionment Approach at a Site Impacted by Multiple Point Sources. *Environ. Sci. Technol.* **2013**, *47*, 3743-3751.
20. Charron, A.; Degrendele, C.; Laongsri, B.; Harrison, R.M. Receptor modelling of secondary and carbonaceous particulate matter at a southern UK site. *Atmos. Chem. Phys.* **2013**, *13*, 1879-1894.
21. Marmur, A.; Unal, A.; Mulholland, J. A.; Russell, A. G. Optimization-based

source apportionment of PM2.5 incorporating gas-to-particle ratios. *Environ. Sci. Technol.* **2005**, *39*, 3245-3254.

22. Cheng, H.; Gong, W.; Wang, Z.; Zhang, F.; Wang, X.; Lv, X.; Fu, X.; Liu, J.; Zhang, G. Ionic composition of submicron particles (PM 1.0) during the long-lasting haze period in January 2013 in Wuhan, central China. *J. Environ. Sci.* **2014**, *26*, 810-817.

23. Kerminen, V. M.; Hillamo, R.; Teinila, K.; Pakkanen, T.; Allegrini, I.; Sparapani, R. Ion balances of size-resolved tropospheric aerosol samples: implications for the acidity and atmospheric processing of aerosols. Atmos. Environ. **2001**, *35*, 5255-5265.